Ecological Modelling 266 (2013) 131–143

Contents lists available at ScienceDirect

Ecological Modelling

journal homepage: www.elsevier.com/locate/ecolmodel

Assessing potential climate change effects on vegetation using a linked model approach

Jessica E. Halofsky[a,*], Miles A. Hemstrom[b], David R. Conklin[c], Joshua S. Halofsky[d], Becky K. Kerns[e], Dominique Bachelet[c]

[a] School of Environmental and Forest Sciences, University of Washington, Box 352100, Seattle, WA 98195-2100, USA
[b] USDA Forest Service, Forestry Sciences Laboratory, 620 SW Main St., Suite 400, Portland, OR 97205, USA
[c] Conservation Biology Institute, 136 SW Washington Avenue, Suite 202, Corvallis, OR 97333, USA
[d] Washington Department of Natural Resources, PO Box 47000, 1111 Washington Street SE, Olympia, WA 98504-7000, USA
[e] USDA Forest Service, Forestry Sciences Laboratory, 3200 SW Jefferson Way, Corvallis, OR 97331, USA

ARTICLE INFO

Article history:
Received 21 February 2013
Received in revised form 14 June 2013
Accepted 1 July 2013

Keywords:
Climate change
Dynamic global vegetation models
State-and-transition models
Vegetation dynamics
Wildfire

ABSTRACT

We developed a process that links the mechanistic power of dynamic global vegetation models with the detailed vegetation dynamics of state-and-transition models to project local vegetation shifts driven by projected climate change. We applied our approach to central Oregon (USA) ecosystems using three climate change scenarios to assess potential future changes in species composition and community structure. Our results suggest that: (1) legacy effects incorporated in state-and-transition models realistically dampen climate change effects on vegetation; (2) species-specific response to fire built into state-and-transition models can result in increased resistance to climate change, as was the case for ponderosa pine (*Pinus ponderosa*) forests, or increased sensitivity to climate change, as was the case for some shrublands and grasslands in the study area; and (3) vegetation could remain relatively stable in the short term, then shift rapidly as a consequence of increased disturbance such as wildfire and altered environmental conditions. Managers and other land stewards can use results from our linked models to better anticipate potential climate-induced shifts in local vegetation and resulting effects on wildlife habitat.

1. Introduction

Climate, in concert with local topoedaphic factors, dictates vegetation distribution through thermal and water constraints on plant regeneration, establishment, growth, and mortality. Global vegetation patterns are already shifting in response to observed increases in temperature and changing precipitation patterns (Parmesan, 2006; Allen et al., 2010). Anticipating potential shifts in local vegetation is critical for land managers to develop adaptive strategies. However, predicting vegetation response to climate change requires consideration of interacting physical and biological processes at multiple spatial and temporal scales. Dynamic global vegetation models (DGVMs) are currently considered to be among the most advanced tools to assess climate change effects on ecosystems (Fischlin et al., 2007). DGVMs integrate state-of-the-art knowledge of plant physiology, biogeography, biogeochemistry, and biophysics, with climate model projections to simulate changes in vegetation structure and composition (biogeography) as well as ecosystem function (biogeochemistry) through time (Prentice et al., 1989, 2007; Foley et al., 1998; Cramer et al., 2001). MC1 (Daly et al., 2000; Bachelet et al., 2001) is a DGVM that integrates biogeography, biogeochemistry, and fire into a single modeling environment and has been used for regional- to global-scale assessments of potential climate change effects on ecosystems (e.g., Bachelet et al., 2000, 2003; Lenihan et al., 2008a,b; Gonzalez et al., 2010; Rogers et al., 2011; Shaw et al., 2011). DGVMs simulate broad plant functional types that combine numerous species into single entities (e.g., evergreen needleleaf trees), and thus they are incapable of simulating community- and species-level changes at the landscape scale (Hickler et al., 2004). However, because they focus on mechanisms, their projections of future outcomes are more reliable than simple correlations of location with current climate conditions. To take full advantage of their strength, their results can be translated into directions and magnitude of change applicable to community- and species-level dynamics, making output more useful for sub-regional management and planning efforts (e.g., Halofsky et al., 2011).

State-and-transition models (STMs) simulate trends in vegetation community response to a variety of local disturbances and management strategies by explicitly incorporating landscape legacy, succession rules and species-specific sensitivity to disturbance. STMs are based on transition matrix methods that simulate

* Corresponding author. Tel.: +1 206 543 9138.
E-mail address: jhalo@uw.edu (J.E. Halofsky).

0304-3800/$ – see front matter © 2013 Elsevier B.V. All rights reserved.
http://dx.doi.org/10.1016/j.ecolmodel.2013.07.003

vegetation dynamics using transition probabilities between vegetation states (e.g., Horn, 1975; Noble and Slatyer, 1980; Westoby et al., 1989; Laycock, 1991). The landscape is divided into states representing combinations of cover type (dominant species) and structural stage (e.g., diameter class, canopy density, and number of canopy layers) within a particular biophysical environment. For example, a state could represent dry ponderosa pine forest in the 25–38 cm diameter class with closed tree canopy and a single canopy layer. States are linked by transitions that represent natural disturbances, management actions, or successional processes. For example, high-severity fire could drive a ponderosa pine forest, 25–38 cm diameter class, closed-canopy state to an open grassland state. STMs are run at scales appropriate for management and planning efforts (units typically range from 10 s to 1000 s of ha in size). They have been extensively used for regional to sub-regional assessments (e.g., Hemstrom et al., 2001, 2002, 2007; Merzenich et al., 2003; Forbis et al., 2006; Weisz et al., 2009). However, with the exception of some very recent developments (Provencher and Anderson, 2011), STMs have not incorporated the effects of climate change.

Here we present results from a novel modeling approach that links the mechanistic power of a DGVM with the community-specific control of state-and-transition models to project local vegetation shifts. We linked a DGVM (MC1) with a set of eight STMs, each representing a major vegetation type in a study area in central Oregon, to assess potential changes in species composition and community structure under different climate change scenarios. Our objectives are to (1) describe the approach we used to link the DGVM with STMs; and (2) project potential future changes in species composition and community structure for the central Oregon study area.

2. Materials and methods

2.1. Study area

The study area is a landscape of forests, woodlands, shrublands, and grasslands that is 1,023,808 ha in size, located in central Oregon, USA (Fig. 1). Elevations vary from about 1200 m to above 2400 m. The climate is transitional between moist, maritime conditions west of the Cascade Mountains (which are oriented north to south; Fig. 1) and continental conditions to the east. Annual precipitation varies from over 2000 mm along the Cascade Crest to less than 350 mm along lower treeline and 250 mm at the lowest elevations in shrub-steppe environments (PRISM Group, 2012). Most of the precipitation falls as rain and snow during the winter months, with snow packs of more than 2 m common in upper elevations. Summers are warm and dry, often with several weeks of very low or no precipitation and warmest temperatures at lower elevations exceeding 30 °C.

2.2. The MC1 model

MC1 (Bachelet et al., 2001) is a DGVM that simulates: life-form mixtures, classifying them into potential vegetation classes (PVCs); the fluxes and pools of carbon, nitrogen, and water through ecosystems; and natural fire occurrence and effects. MC1 routinely generates century-long, local to global-scale simulations (e.g., Bachelet et al., 2003; Daly et al., 2000; Lenihan et al., 2003, 2008a; Hayhoe et al., 2005; Rogers et al., 2011). The model reads soil and monthly climate data, and calls interacting modules that simulate biogeography, biogeochemistry, and fire disturbance.

The biogeography module, which was developed using some of the biogeography rules from the MAPSS model (Neilson, 1995), simulates life-form mixtures of evergreen needleleaf or broadleaf, and deciduous needleleaf or broadleaf trees, as well as temperate (C3) and warm-season (C4) grasses. An algorithm is used to determine life-form mixture at each annual time-step as a function of annual average minimum monthly temperature and growing season precipitation (see Bachelet et al., 2001; Daly et al., 2000). Tree and grass life-form mixtures, their biomass simulated by the biogeochemistry module, as well as climate indices are used to determine which of several dozen possible PVCs occurs in each simulated grid cell each year (see Bachelet et al., 2001; Daly et al., 2000).

The biogeochemistry module is a modified version of the CENTURY model (Parton et al., 1993), which simulates plant growth, organic matter decomposition, and the movement of water and nutrients through ecosystems. The biomass and hydrology algorithms from CENTURY were retained and linked to the dynamic biogeography driver. Life-form specific parameters (e.g., maximum production rate of evergreen trees) are determined annually by modifying their original values as a function of their dominance along the two-dimensional climatic gradient defined by growing season precipitation and annual average minimum monthly temperature (Bachelet et al., 2001). In this study, plant growth was assumed not to be limited by nutrient availability; the nitrogen

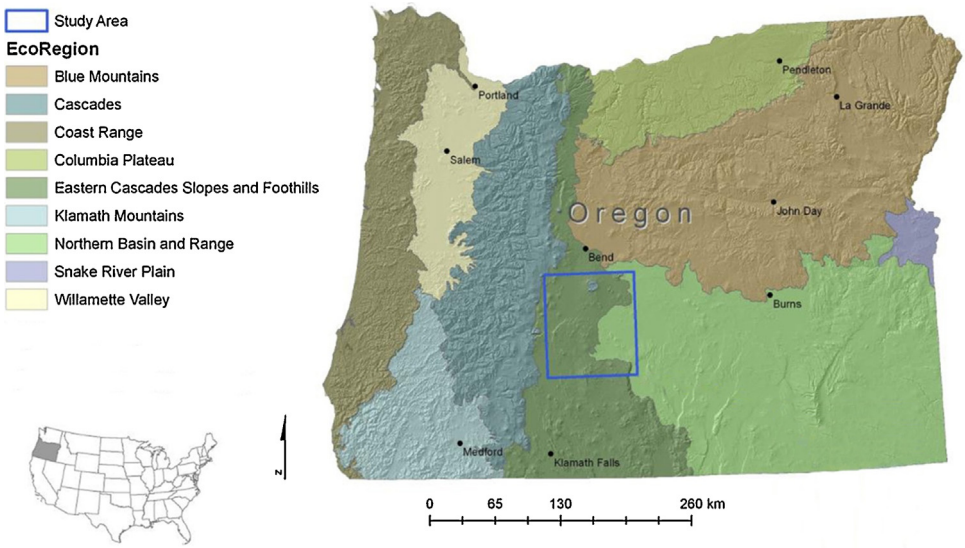

Fig. 1. Study area in central Oregon, USA. Ecoregions shown are Omernik Level III Ecoregions (Omernik, 1987).

demand was estimated and met assuming biological nitrogen fixation would provide what deposition did not. The direct effect of the observed increase in atmospheric carbon dioxide (CO_2) concentration was simulated using a beta factor (Friedlingstein et al., 1995) that increases maximum potential productivity and reduces the moisture constraint on productivity. Grasses compete with woody plants for soil moisture and nutrients in the upper soil layers where both are rooted, while the deeper-rooted woody plants have sole access to water in deeper layers. The growth of grasses is also limited by reduced light levels due to increased plant density as well as shading by woody plants.

The MC1 fire module (Lenihan et al., 1998) simulates the occurrence, behavior, and effects of fire in all PVCs. The model simulates fire initiation and the behavior of a fire event in terms of the potential rate of fire spread, fireline intensity, and the transition from surface to crown fire (Rothermel, 1972; van Wagner, 1973; Cohen and Deeming, 1985). Estimates of fuel bed characteristics are required to simulate fire behavior, and are provided by the other two MC1 modules. The current life-form mixture is used to select factors that allocate the simulated live and dead carbon pools into classes of live fuels (grass leaves) and dead fuels (1-h [<0.64 cm diameter], 10-h [0.64–2.54 cm diameter], 100-h [2.54–7.6 cm diameter], and 1000-h [7.6–20.3 cm diameter]). The moisture content of the live fuels is derived from soil moisture calculated in the biogeochemistry module. Dead fuel moisture content is estimated from the climate drivers using different functions for each of four dead fuel size-classes (Cohen and Deeming, 1985).

Fire events are initiated in the model when the fine fuel moisture drops below a defined threshold and fuel buildup simultaneously exceeds a defined threshold. Sources of ignition (e.g., lightning) are assumed to be always available. Area burned is not simulated explicitly as fire spread within a given cell (potential rate of fire spread, mentioned above, is used to determine plant mortality and fuel consumption); instead, the fraction of a cell burned by a fire event is estimated as a function of set minimum and maximum fire return intervals for the dynamically-simulated PVC and the number of years since the last simulated fire event (Lenihan et al., 2008a). The fire effects simulated by the model include plant mortality and consumption of vegetation carbon, which is removed from (or transferred to) the appropriate carbon pools in the biogeochemistry module. Fire-driven mortality and consumption are simulated as a function of fireline intensity and tree canopy structure (Peterson and Ryan, 1986). Dead biomass consumption is simulated using functions of fuel moisture that are fuel-class specific (Anderson et al., 2005). See Bachelet et al. (2001) for additional information on general MC1 model formulation and parameterization.

2.3. Climate projections

Climate data sets required for running the MC1 model in this study consisted of monthly values of four variables: precipitation, the monthly means of diurnal extreme temperatures, and a measure of atmospheric water content. For the historical period, we used the PRISM (Parameter–elevation Relationships on Independent Slopes Model) climate data set on a 30-arcsec grid (~800 m grain; Daly et al., 1997, 2008). The PRISM group provided monthly data for the years 1895–2008 for the conterminous U.S. Three future climate projections from general circulation models (GCMs) included in the World Climate Research Programme's (WCRP's) Coupled Model Intercomparison Project phase 3 (CMIP3) multi-model dataset and subsequently in the Intergovernmental Panel on Climate Change (IPCC) Fourth Assessment Report (IPCC, 2007) were used to drive MC1 projections for the 21st century. We obtained complete time series of the four necessary climate variables from the data repository at Lawrence Livermore Laboratories produced by the MIROC 3.2 medres (Hasumi and Emori, 2004), CSIRO Mk3 (Gordon et al., 2002), and Hadley CM3 (Gordon et al., 2000; Johns et al., 2003) GCMs (hereafter MIROC, CSIRO, and Hadley, respectively) for the IPCC SRES A2 emissions scenario (Nakićenović and Swart, 2000). We used the A2 carbon dioxide emissions scenario. A full century transient series from 2010 to 2100 was used as input to MC1.

Mote and Salathé (2010) compared projections from 21 GCMs used in the IPCC AR4 to historical climate data (University of East Anglia Climatic Research Unit version 2.02; Mitchell et al., 2004) for the Pacific Northwest over the 1970–1999 period. Compared to the other models assessed by Mote and Salathé (2010), Hadley produced a relatively low precipitation bias (or mean difference between model projections and historical climate data; both annually and seasonally), but failed to show an increasing trend in mean annual temperature over the 20th century. MIROC showed a relatively low temperature bias but high precipitation bias. CSIRO was ranked highest for reproducing the trend in mean annual temperature over the 20th century, but had a high positive temperature bias.

For the U.S. Pacific Northwest, CSIRO projects a relatively cool and wet future conditions (+2.6 °C and +176 mm mean annual precipitation in 2070–2099), MIROC projects relatively hot and wet conditions (+4.2 °C and +82 mm mean annual precipitation in 2070–2099), and Hadley projects relatively hot and dry conditions (+4.2 °C and −78 mm mean annual precipitation in 2070–2099) (Rogers et al., 2011). For all three GCMs, temperature increases are generally greater in summer than in winter, while precipitation increases in winter and decreases in summer. Mean monthly summer (June, July, August) precipitation decreases by as much as 5 mm under CSIRO, 10 mm under MIROC, and 15 mm under Hadley, with historical mean monthly summer precipitation of 30–50 mm over most of Oregon and Washington (Rogers et al., 2011).

The spatial grids used by the MIROC, CSIRO, and Hadley GCMs are coarse (2.8×2.8 degrees for MIROC, 1.9×1.9 degrees for CSIRO, and 2.5×3.75 degrees for Hadley). We down-scaled the coarse grid GCM data to a 30-arcsec grid using a "delta" or "anomaly" method (Fowler et al., 2007). We first calculated a historical climate baseline (mean values for each month) for 1971–2000, our reference period, using PRISM data. We also calculated a coarse-scale historical baseline for the same reference period using the GCM projections. Secondly, for each month of each year of the future period, we calculated the difference (for temperature and vapor pressure) or the ratio (for precipitation) of the future value and the reference historical baseline climate from each GCM (the "delta"). We then down-scaled the coarse-scale deltas to the fine (30-arcsec) grid using bilinear interpolation. Finally, we calculated the fine grid climate values for each month of each year of the future period using the PRISM historical baseline modified by the fine-scale deltas (meaning that topographic effects are incorporated in the down-scaled climate data to the extent that they are represented in the PRISIM data). Difference deltas were added to the baseline while ratio deltas were multiplied with the baseline.

2.4. State-and-transition models (STMs)

The STM approach characterizes vegetation in terms of states that are linked together by transitions, which describe processes that cause change among vegetation states (Westoby et al., 1989; Laycock, 1991). We used, and in some cases modified, previously-developed STMs for our study area (Hann et al., 1997; The Nature Conservancy, 2006; Hemstrom et al., 2007; Evers, 2010). Existing STMs were developed in the Vegetation Development Dynamics Tool (VDDT; ESSA Technologies Ltd., 2007). VDDT is stand-alone software that allows development of STMs and simulates vegetation dynamics by dividing the landscape into states, assigning probabilities to transitions between states, and simulating the state

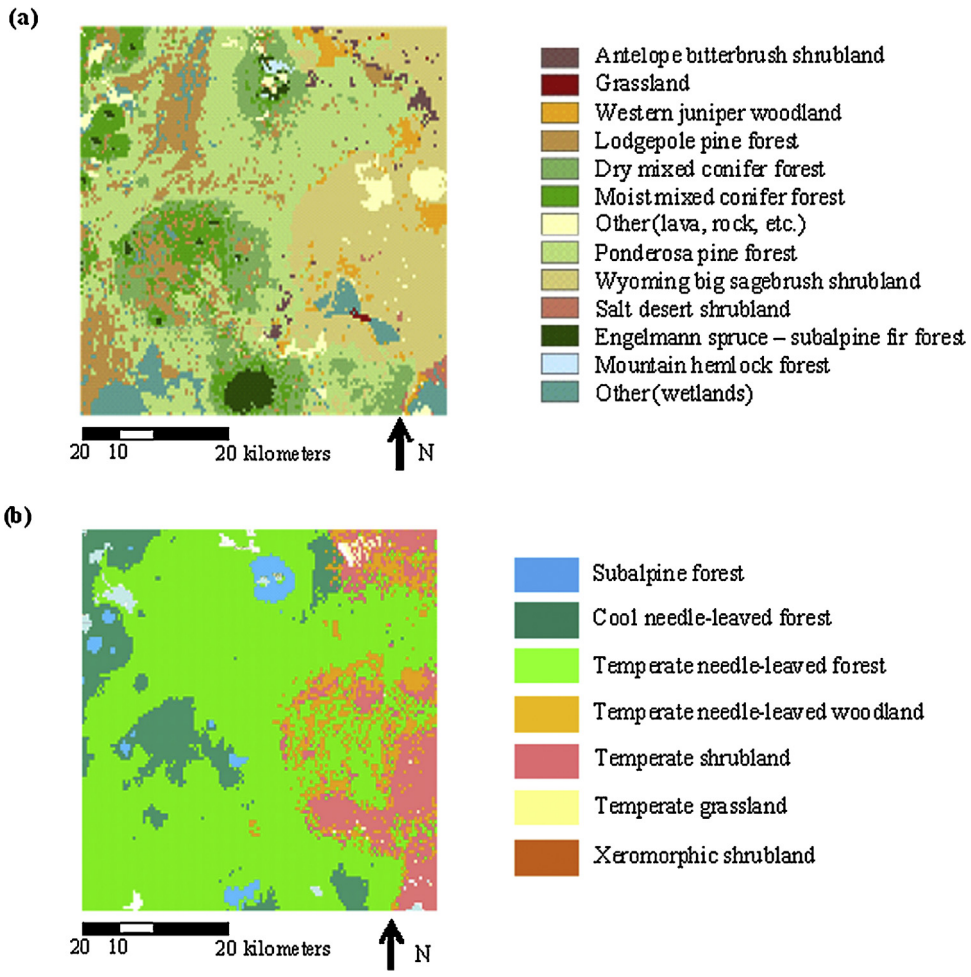

Fig. 2. (a) Potential vegetation types mapped from imputation of inventory plots, and (b) potential vegetation classes simulated by MC1 for the recent historical period (1971–2000). We matched the potential vegetation types in (a) to corresponding vegetation classes in (b) using spatial overlays. In cases where a single potential vegetation class corresponded with multiple potential vegetation types, we chose the most spatially extensive potential vegetation type within the potential vegetation class area.

of the landscape over time using Monte Carlo methods. Transitions between states may be either deterministic or probabilistic. Deterministic transitions are specified to occur after a certain number of time steps within a state (e.g., succession), whereas probabilistic transitions are defined by an annual transition probability (e.g., wildfire). Recently, VDDT was folded into the Path interface (ApexRMS and ESSA, 2011), which has improved model building and analysis features and facilitates running spatially-explicit STMs. Thus, model simulations were run using the Path modeling platform using annual time-steps.

The previously-developed set of STMs used for this study included 11 STMs, each representing a single potential vegetation type (PVT; Fig. 2a). However, to incorporate climate-induced changes in vegetation from MC1 in the STMs, we chose a representative STM for each PVC that was simulated by MC1 in the study area. To choose representative STMs, we used spatial overlays of historical (1971–2000) MC1 results (Fig. 2b) and our maps of current PVT distribution (Fig. 2a), generating a crosswalk table (Table 1). In cases where a single PVC corresponded with multiple PVTs, we chose the most spatially extensive PVT within the PVC area. MC1 simulations for the future showed a new PVC occurring in the study area, warm-season grassland. Thus, we chose an STM from a more southern modeling zone to represent warm-season grassland.

Previously-developed STMs for the study area were independent, meaning that once a given area of land was classified into a certain PVT, represented by a single STM, it could not be reclassified into another PVT over time in the model simulations. Thus, while a given area could move among different states within an individual STM over time due to management, natural disturbances, and vegetation development, that area could not change PVTs. We changed this by modifying the model structure, developing one large interconnected STM, and allowing shifts among PVTs with climate change and disturbance. We assumed that the PVC changes projected by MC1 could be approximated by changes among similar or representative PVTs that currently exist in the study area or occur in adjacent landscapes (Table 1). Our selected PVTs are used to represent future vegetation types that we assume will have generally similar internal vegetation dynamics and disturbance relations.

STMs for forested PVTs (large green boxes in Fig. 3) included states (combinations of vegetation composition and structure; small gray boxes in Fig. 3) defined by overstory cover type and structural conditions. Cover types were defined by the dominant tree species in the upper-most canopy layer. For example, the STM for the ponderosa pine-lodgepole pine PVT included both ponderosa pine and lodgepole pine cover types. Within cover types, structural classes were defined by combinations of tree diameter class (quadratic mean diameter of the largest 20% of the trees; 0 cm Diameter at Breast Height (DBH) = Grass/forb; <13 cm DBH = seedling/sapling; 13–25 cm DBH = pole; 25–38 cm DBH = small; 38–51 cm DBH = medium; 51–76 cm DBH = large; >76 cm DBH = giant), overstory canopy cover (<10% = grass/forb,

Table 1
MC1 potential vegetation classes and their corresponding state-and-transition model (STM) potential vegetation types in the study area. We chose one representative STM for each MC1 potential vegetation class (representative STMs are underlined in the STM potential vegetation type column). Mapped current extent is derived from imputation of inventory plot characteristics across the study area. MC1 current extent represents current conditions as simulated by the MC1 model.

MC1 potential vegetation classes	STM potential vegetation types	Common species	Imputed current extent (%)	MC1 current extent (%)
Subalpine forest	Mountain hemlock and subalpine fir forests	Mountain hemlock (*Tsuga mertensiana*), whitebark pine (*Pinus albicaulis*), Engelmann spruce (*Picea engelmannii*), subalpine fir (*Abies lasiocarpa*), and lodgepole pine (*Pinus contorta*)	2	2
Cool needleleaf forest	Moist mixed conifer forests	Douglas-fir (*Pseudotsuga menziesii*), white fir (*Abies concolor*), Shasta red fir (*Abies* × *shastensis* [*magnifica* × *procera*]), ponderosa pine (*Pinus ponderosa*), western hemlock (*Tsuga heterophylla*), and western redcedar (*Thuja plicata*)	11	4
Temperate needleleaf forest	Ponderosa pine, lodgepole pine, and dry mixed conifer forests	Ponderosa pine, lodgepole pine, Douglas-fir, and grand fir (*Abies grandis*)	59	67
Temperate needleleaf woodland	Mountain big sage—western juniper woodland and shrubland	Western juniper (*Juniperus occidentalis*), and mountain big sagebrush (*Artemisia tridentata* ssp. *vaseyana*)	14	6
Temperate shrubland	Wyoming big sage shrubland	Wyoming big sagebrush (*Artemisia tridentata ssp. wyomingensis*), and antelope bitterbrush (*Purshia tridentata*)	12	18
Xeromorphic shrubland	Salt desert shrubland	Greasewood (*Sarcobatus vermiculatus*), saltbush (*Atriplex canescens*), and Wyoming big sagebrush	2	<1
Temperate grassland	Bluebunch wheatgrass–Sandberg bluegrass grassland	Idaho fescue (*Festuca idahoensis*), bluebunch wheatgrass (*Pseudoroegneria spicata*), and cheatgrass (*Bromus tectorum*) (non-native)	<1	3
Warm-season grassland	Warm-season grassland	Galleta (*Pleuraphis* spp.)	0	0

10–40% = low, 40–60% = medium, >60% = high), and canopy layering (single or multiple). A grass-forb state represented early-successional conditions before establishment of a significant tree canopy. We also included post-disturbance states that resulted from a stand-replacing disturbance (insect outbreak or wildfire) prior to any salvage logging and, consequently, containing standing snags and downed wood. In similar fashion, our STMs for arid land PVTs (all woodlands, shrublands, and grasslands in Table 1) included vegetation states defined by cover types (dominant species composition) and structural conditions. Cover types reflected varying amounts of native, semi-degraded, and exotic herbaceous and shrub states, and different phases of juniper invasion, where applicable. For example, the STM for the Wyoming big sage shrubland PVT included both Wyoming big sage with exotic annual grasses and native perennial grass cover types. Within cover types, structural classes reflected percent cover by life-form (grasses, shrubs, or trees).

To characterize the PVT (Fig. 3a) for each 30-m pixel on the landscape and determine which STM to use for that pixel, we acquired forested PVT maps from ecoshare (http://ecoshare.info/), and arid lands PVT maps were downloaded from the Integrated Landscape Assessment Project website (http://oregonstate.edu/inr/ilap/). To inform initial vegetation conditions (vegetation composition and structure, i.e., states) for each 30-m pixel within a PVT, existing vegetation maps for forests were downloaded from the Landscape Ecology, Modeling, Mapping and Analysis website (LEMMA, http://www.fsl.orst.edu/lemma), and existing vegetation maps for arid lands were downloaded from the Integrated Landscape Assessment Project website (http://oregonstate.edu/inr/ilap/). Both PVT and existing vegetation maps were derived from imputations of the measured vegetation in inventory plots to 30-m pixels using gradient nearest neighbor (Ohmann and Gregory, 2002) and random forest methods (Crookston and Finley, 2007). These methods essentially assign inventory plots and associated data to 30-m pixels as a statistical function of LANDSAT-TM imagery and a variety of topographic, land ownership, and other data. In forested PVTs, each pixel was first assigned a cover type based on the importance value of the dominant tree species (using expert-developed importance value

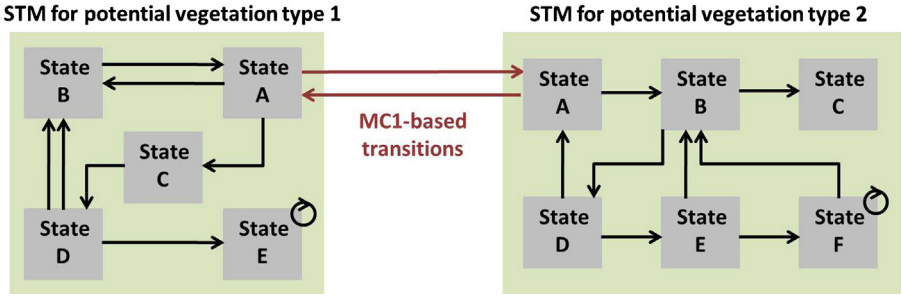

Fig. 3. Simplified illustration of state-and-transition models (STMs; green boxes), each representing a single potential vegetation type, or PVT. STMs are characterized by states (combinations of vegetation composition and structure; gray boxes), with transitions among states (black arrows) representing natural disturbances, management, and succession. To incorporate climate change in our set of previously-independent STMs, we developed one large, interconnected STM that allowed transitions among PVTs based on MC1 vegetation change and fire output (red arrows). Transitions among PVTs only occurred when vegetation was in an early-successional, open condition (here represented by State A). Our actual climate-informed STM included eight potential vegetation types with MC1-based transitions among them. (For interpretation of the references to color in this figure legend, the reader is referred to the web version of this article.)

to cover type crosswalk tables). Then the pixel was assigned to a structural stage based on tree size, percent canopy cover, and number of canopy layers (categories described above). Total existing land area in each PVT-cover-structure combination was then computed to reflect current conditions, and we used that information as the initial conditions for STM runs.

The STMs used in the study included major natural disturbances for the study area, including wildfire (low, mixed, and high severity), insect outbreaks, wind disturbance, and drought mortality. With the exception of fire, disturbance-related transition rates incorporated in the models were developed through expert opinion. We developed empirical wildfire probabilities based on an analysis of wildfire data for the 1984–2008 time period (Monitoring Trends in Burn Severity (MTBS); Eidenshink et al., 2007) in the Oregon East Cascades ecological region. MTBS data includes burn perimeters and burn severity classes for all fires over 405 ha in the western United States over a 25 year time span (1984 to 2008). The 405 ha threshold results in smaller fires being omitted from the analysis, potentially reducing our calculated wildfire probabilities, but since the area covered by these <405 ha fires is relatively small at the scale of large landscapes, the effect of not including these fires in the analysis was likely minor. To obtain wildfire probabilities for STMs, MTBS burn perimeter polygons were overlaid in a Geographic Information System with our PVT map. We classified each PVT into one of five fire regime categories (dry forests, moist forests, high-elevation forests, semi-desert shrub steppe, mesic shrub steppe). We then calculated the number of hectares burned each year for each PVT category. Annual fire probabilities were obtained by dividing the number of hectares burned in each potential vegetation group by the size of the area in the potential vegetation group. These annual values became the wildfire probabilities in our models. While we used empirical data to determine fire return intervals for each PVT, we did not modify the expert-derived values representing the proportion of each state burning at different wildfire severities.

STMs for each PVT were built as separate entities. However, to allow shifts among PVTs, we constructed one large, interconnected STM that aggregated all the selected STMs for the study area (e.g., Fig. 3). We then added transitions to allow a given area of land to be reclassified into a different PVT according to PVC transition rates simulated by MC1 under the selected climate change scenarios (see Section 2.5 for more detail). Thus, we built one interconnected "climate-informed" STM (climate-informed STM hereafter).

Although effects of management can be explicitly incorporated in STM simulations, for the purpose of illustrating the process of incorporating climate change in STMs, we did not include management in our simulations.

2.5. MC1–STM integration

To incorporate changes in vegetation from MC1 in our large, interconnected STM, we identified PVC changes simulated by MC1 between 2010 and 2100 for three climate change scenarios (MIROC-A2, CSIRO-A2, and Hadley-A2), and used the PVC changes from MC1 under the three climate scenarios to inform probability of PVT changes in the STM (meaning the STM was run under three different scenarios of climate and vegetation change). We selected only those PVC changes that affected at least 1% of the study area over the 2010–2100 time period. We calculated the average probability for each selected PVC change by dividing the area in which the PVC change occurred each year by the total area of the study region, yielding a percent of the study area in which that PVC change occurred for annual timesteps, and averaging the area percentages for each change across all years. Average probabilities for PVC changes were incorporated in the interconnected STM as transitions that lead from post-disturbance and early-successional states of a source PVT to the same (or functionally similar) structural state in a different PVT. We assumed that these new climate change transitions would occur from open vegetation states or following stand-replacing disturbances. Thus, when an area of vegetation was simulated to be in an open or post-stand-replacing disturbance state in a given PVT, there was a certain probability of that area shifting to each of the other PVTs based on MC1 output (in some cases that probability would be zero, depending on the PVT to PVT shift). Whether a shift actually occurred depended on the "roll of the dice" in the Monte Carlo simulations.

In addition to incorporating the average probabilities for each PVC change across the entire MC1 simulation, we incorporated the trends in magnitude of those changes over time in the MC1 simulation through the use of trend multipliers in the STM. We computed the annual departure of each PVC transition from the mean change (across the entire simulation) for that transition. For each year simulated by MC1, a trend multiplier indicated how much the PVC trend was above or below the average trend across the entire simulation. This method allowed us to track in our STM the year-to-year changes in PVCs simulated by MC1. The trend multipliers were applied to scale the proportional annual movement of area among the relevant states and PVTs in the STM. Thus, although PVC changes occur in individual cells in MC1, we did not translate the finer-scale spatial patterns in PVC changes into the STM, but rather incorporated broader landscape-scale trends in PVC changes into the STM.

We used MC1 projections for annual fraction of grid cells burned for each climate scenario in the study area to apply climate-induced changes in fire probabilities in our STM. Patterns in annual area burned for forested and arid land vegetation types were analyzed separately. Since MC1 was run without fire suppression, projections for historical area burned from MC1 were higher than records indicated had historically burned in the area given fire suppression (Westerling et al., 2006; Littell et al., 2010). Similarly, under future climate projections, future fire amounts from MC1 were likely higher than what might actually occur given our expectation that fire suppression will continue in the future. We compensated for the lack of fire suppression in the MC1 model by using an empirical data set (MTBS) from the fire suppression era (1984–2008) to scale MC1 fire area burned projections (equally across the entire simulation period). We compared MTBS area burned observations to historical area burned simulated by MC1 over the 1984–2008 period. We assumed differences were due to fire suppression and adjusted the multipliers to scale future projections of fire area burned from MC1 accordingly.

In addition to trend values, we used the scaled future projections of area burned to create another layer of annual temporal multipliers called Monte Carlo multipliers (MCMs). MCMs were created for each climate scenario for both forest and arid lands. MCM values represent randomized sequences of numbers which reflect that some years are characterized by more natural disturbance than others. To create wildfire MCM values, we first ordered the scaled future projections of area burned from smallest to largest. We then ranked the values for the 90-year MC1 projection. Those values ranking in the 0–80th percentile represented a normal fire year in terms of area burned, while those values in the 80–95th percentile represented severe fire years, and the remaining values represented extreme fire years. We then averaged and normalized those values within each category to create our wildfire MCM multipliers. Normalizing the values ensured the overall fire return interval assigned to the PVT was constant over the simulation period. Once the MCM multipliers were generated, we ran the climate-informed STM with 30 Monte Carlo simulations for each climate scenario, and ran each simulation for 90 years (for the 2010 to 2100 time period) with annual time-steps.

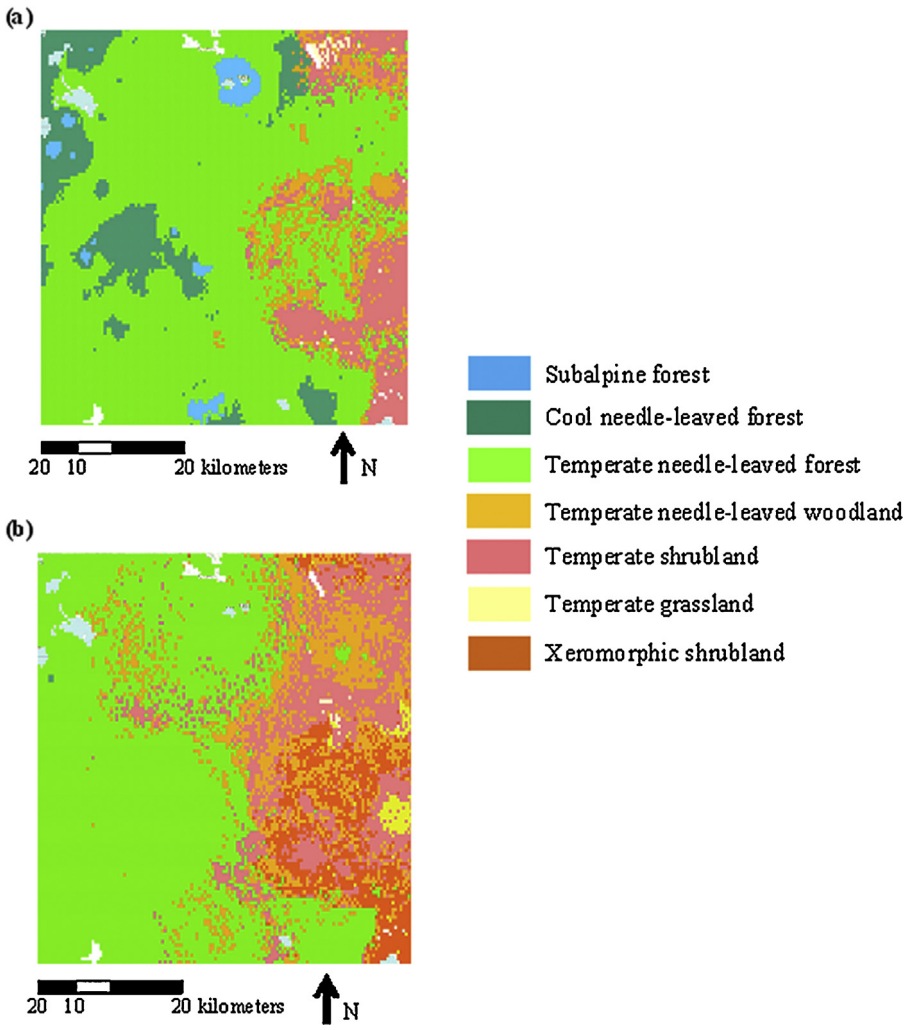

Fig. 4. Potential vegetation class simulations from MC1 for (a) recent historical (modal vegetation class over the 1971–2000 period) and (b) future (2100) under the MIROC general circulation model climate change projections for the A2 emissions scenario.

3. Results

3.1. Historical period potential vegetation and wildfire—MC1 simulation results

Temperate needleleaf forests were the simulated dominant PVC for the study area for the entire historical period (Fig. 4a). However, percent of the landscape simulated as temperate needleleaf forest varied over time; temperate needleleaf forests were simulated to occupy from 50% to 70% of the area over the thirty year historical period. This agreed reasonably well with our maps of existing vegetation for the study area in which the corresponding ponderosa pine/lodgepole pine forests occupied about 59% of the landscape area (Table 1). In addition to temperate needleleaf forests, MC1 projected significant amounts of cool needleleaf forests, subalpine forests, temperate shrublands, and temperate needleleaf woodlands (Fig. 4a), but area simulated in each of these PVCs varied over time. Landscape area simulated as temperate grasslands varied over time, but was generally minor. Neither historical simulations nor current vegetation maps showed significant areas of xeromorphic shrublands or warm-season grasslands. These simulated values also compared well with our estimated current conditions (Table 1).

For the historical period, MC1 simulated mean annual area burned of 0.01% for forests and 0.09% for arid lands. Area burned in any single year over the historical period did not exceed 7% of forested area and 15% of the study area in arid lands.

3.2. Future vegetation conditions—MC1 simulation results

MC1 simulation results varied among climate scenarios, but many overall trends were similar (Figs. 4b and 5). For example, simulated area of temperate needleleaf forests decreased mid- to late-century under all three scenarios, but temperate needleleaf forests composed at least 50% of the landscape by the end of the century under all three climate scenarios. Simulated area of subalpine and cool needleleaf forests declined by the end of the century under all three scenarios. Temperate needleleaf woodlands increased in area mid-century under all three scenarios, but then declined to 10% of the landscape under the MIROC and Hadley scenarios. Simulated area of temperate shrublands was highly variable under all three scenarios, with large mid-century increases in area but sharp declines late in the century. Temperate grasslands similarly expanded by mid-century under all three scenarios, and then declined to <5% by the end of the century. Xeromorphic shrublands increased in the late part of the century under all three scenarios. Warm-season grasslands were simulated to occur in the study area under all three scenarios by mid- to late-century, with negligible (<1%) area under all but the Hadley scenario, under which simulated area was almost 10% of the landscape by late-century.

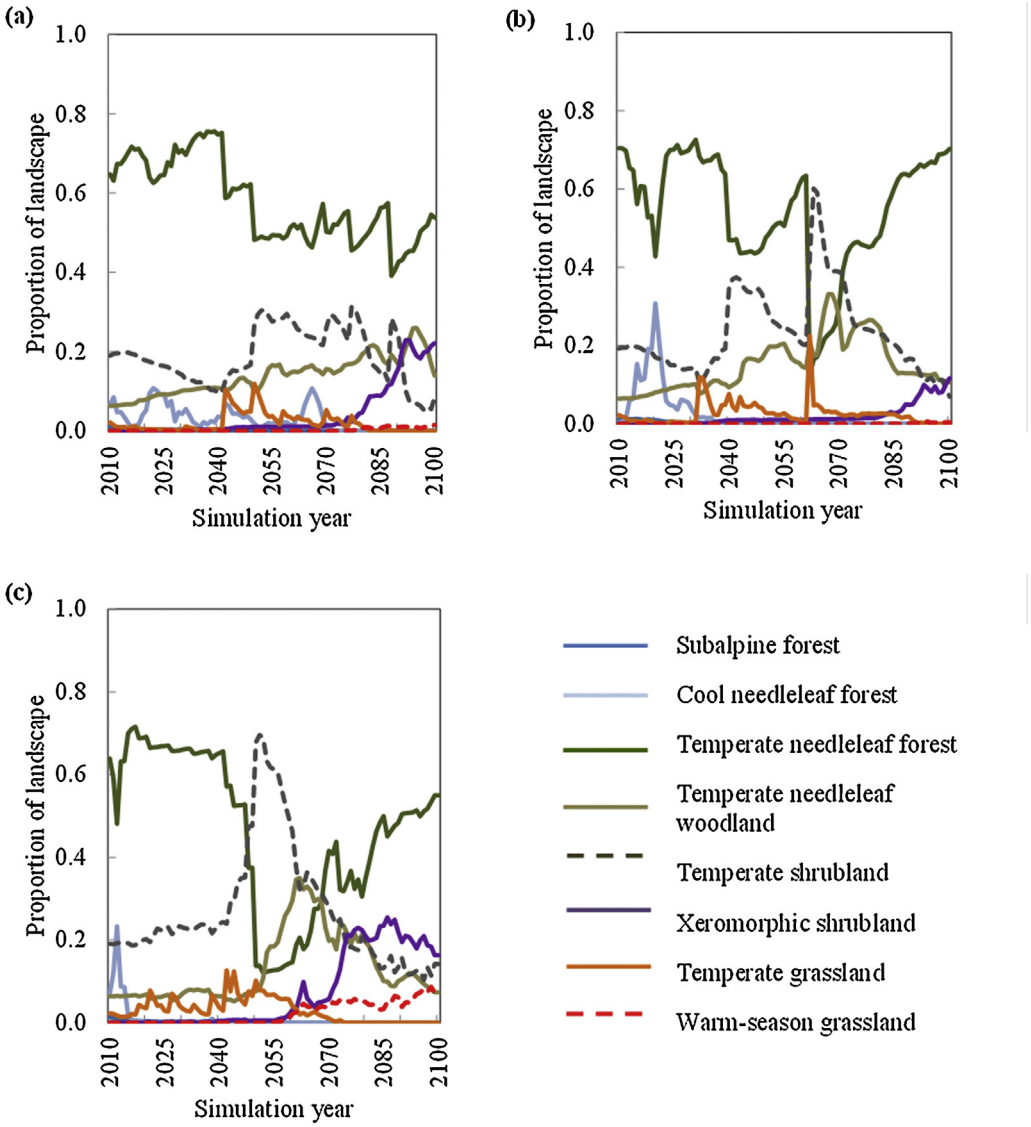

Fig. 5. MC1 projections of annual extent of selected vegetation types using (a) MIROC, (b) CSIRO, and (c) Hadley general circulation model climate projections under the A2 emissions scenario.

3.3. Future wildfire—MC1 simulation results

The MIROC-A2 scenario produced highly variable wildfire in arid lands with fires burning over 80% of the study area several times between 2040 and 2100 (Fig. 6a). Wildfire frequency and extent increased over time in forested lands, but amounts were generally much lower than those in arid lands. The relatively cool and wet CSIRO-A2 simulation generated lower frequency and extent of wildfire in both forested and arid lands (Fig. 6b). Wildfire burned less than 20% of forest lands in most years, but often more than 50% of arid lands. Interestingly, the greatest single wildfire event for both forests and arid lands and in any climate change scenario occurred just after 2060 in the CSIRO-A2 simulation, when nearly all the landscape area burned (Fig. 6b). On average, future wildfires burned the most area under the relatively hot and dry Hadley-A2 scenario, especially in forests (Fig. 6c). Wildfire burned more than three-quarters of forested lands several times between 2070 and 2100. Wildfire in arid lands was higher in early decades, compared to that in forested lands, and burned more than three-quarters of the area several times in the fourth decade, then declined somewhat.

3.4. Future vegetation conditions—STM simulation results

Under the relatively hot and wet MIROC-A2 scenario, the temperate needleleaf forest PVT dominated the study area, though temporal variation in extent increased, especially in the last two decades (Fig. 7a, Table 2). Both cool needleleaf forests and subalpine forests declined by 2100. There was significant expansion of xeromorphic shrublands, which were absent until the last three decades, then increased to nearly 20% of the area. Temperate needleleaf woodlands slowly increased to 20% of the landscape, but declined sharply in the last decade. Simulated area of temperate shrublands and temperate grasslands fluctuated over time, but area in both declined by 2100. Warm-season grasslands were never present in any significant amount.

In the relatively cool and wet CSIRO-A2 scenario, temperate needleleaf forests increased in dominance (Fig. 7b, Table 2), but experienced wide temporal variation in extent in the sixth and seventh decades following very large wildfire episodes in the sixth decade. Cool needleleaf forests and subalpine forests declined by 2100. Temperate needleleaf woodlands increased to >20% of the area in the sixth decade, then declined to about 10% by the end of

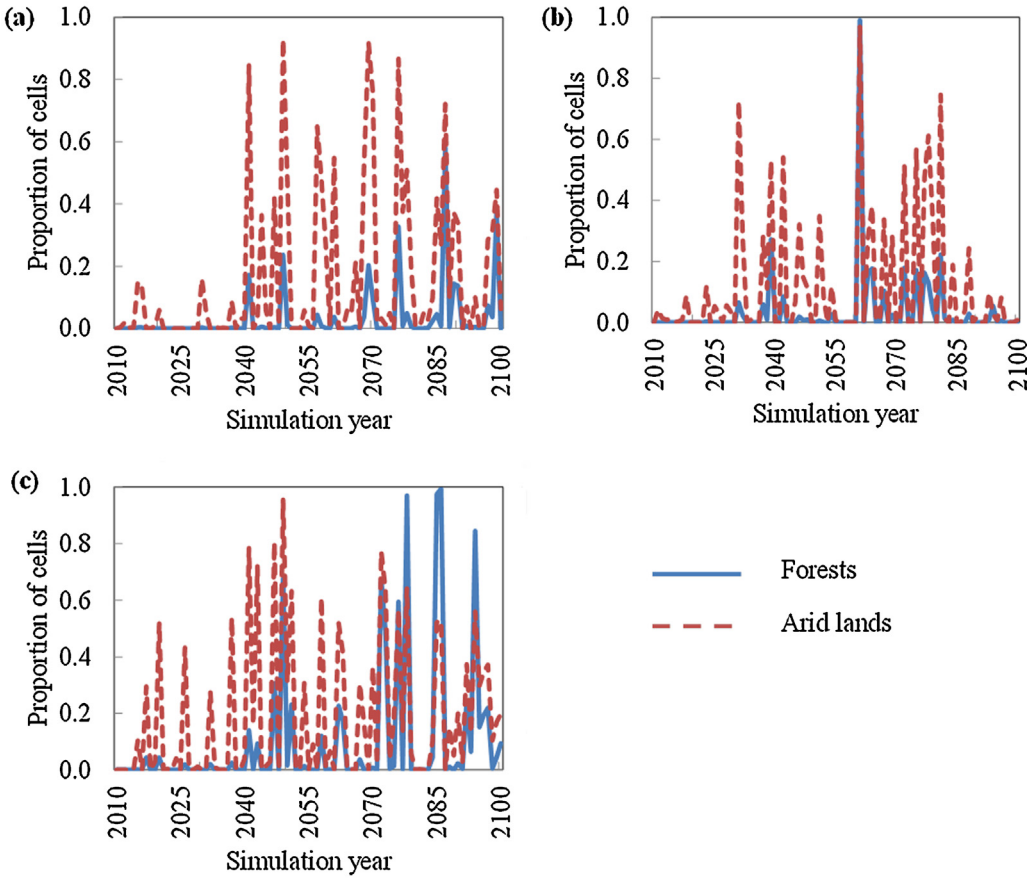

Fig. 6. Simulated future annual area burned as a fraction of the study area simulated by the MC1 model using (a) MIROC, (b) CSIRO, and (c) Hadley general circulation model climate projections under the A2 emissions scenario. Historical mean annual percent of the study area burned was 0.01% for forests and 0.09% for arid lands, respectively.

the simulation. Area of temperate shrublands was highly variable over time, rising to nearly one-third of the area in the sixth decade, and then declining to about 5% by 2100. Xeromorphic shrublands were minor until the last two decades then increased to >5% by 2100. Temperate grasslands increased in area to over 5% in the third and sixth decades, but were otherwise nearly absent. Warm-season grasslands were never present in any significant amounts.

Future vegetation under the hot and dry Hadley-A2 scenario was relatively stable until the fourth decade (Fig. 7c, Table 2), when very large wildfire episodes burned extensive areas in both the forests and arid lands (Fig. 6c). Temperate needleleaf forests were reduced to less than 40% of the landscape area following those events, then began a slow recovery to 60% by the end of the simulation period. Cool needleleaf and subalpine forests declined by the end of the simulation period. Area of temperate needleleaf woodlands was relatively constant until mid-century, increased to over one-quarter of the area by the end of the fifth decade, then decreased to <10% by 2100. Area of temperate shrublands was also relatively constant until the fourth decade, then increased sharply to over 40% of the area by the end of the fifth decade before beginning a steady decline to <10% by the end of the simulation period. Xeromorphic shrublands were nearly absent until mid-century, then increased steadily to >20% of the area by 2100. Temperate grasslands were never very abundant and declined after the sixth decade. Warm season grasslands were absent until 2060, when they increased to about 5% by the end of the simulation.

In sum, all three climate change scenarios projected by our climate smart STM suggested continued dominance of temperate needleleaf forests in our study area (Table 2). All three also forecast declines of cool needleleaf and subalpine forests. All three agreed that temperate needleleaf woodlands will likely remain an important arid-lands vegetation community and that temperate shrublands will likely decline by the end of the century. Temperate grasslands seemed likely to remain minor components of the area, possibly increasing temporarily in middle decades. All three models forecast increasing abundance of xeromorphic shrublands with

Table 2
Initial (current) and projected future (2100) landscape composition of potential vegetation types under the MIROC, CSIRO, and Hadley general circulation model climate projections for the A2 emissions scenario, as projected by climate-informed state-and-transition models.

Potential vegetation type	Initial conditions (%)	MIROC (%)	CSIRO (%)	Hadley (%)
Subalpine forest	2	<1	<1	<1
Cool needleleaf forest	11	3	2	<1
Temperate needleleaf forest	59	59	74	60
Temperate needleleaf woodland	14	13	11	7
Temperate shrubland	12	3	4	8
Xeromorphic shrubland	2	20	9	20
Temperate grassland	<1	0	<1	0
Warm-season grassland	0	1	<1	4

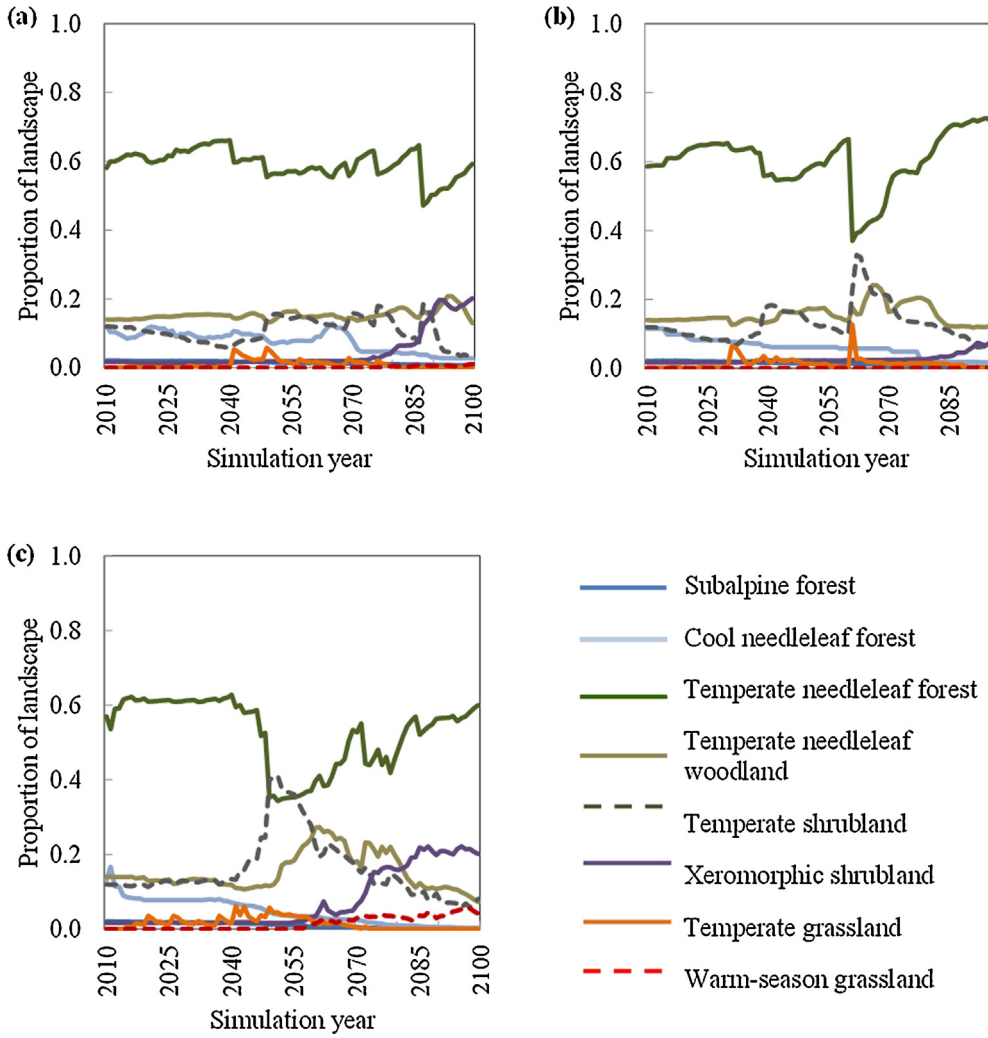

Fig. 7. Climate-informed state-and-transition model simulation of potential future potential vegetation type trends for (a) MIROC, (b) CSIRO, and (c) Hadley general circulation model climate projections under the A2 emissions scenario. Lines represent the mean of 30 Monte Carlo simulations for each climate scenario.

the hot and dry Hadley-A2 scenario showing that they may become the dominant arid-land vegetation community by the end of the century. The Hadley-A2, and to a lesser extent the MIROC-A2, scenarios suggest increasing abundance of warm-season grasslands, which are currently not present. Overall, linked DGVM-STM model simulations under these three climate scenarios suggest that, at the end of the century, central Oregon will have a landscape with at least half its area in ponderosa pine forests and arid lands dominated by either temperate needleleaf woodlands or xeromorphic shrublands, with reduced area of temperate shrublands.

4. Discussion

We have shown how projections of vegetation shifts from the MC1 DGVM (Fig. 5) differ from those produced by a climate-informed STM (Fig. 7). For example, the climate-informed STM (Fig. 7) showed much less variability in the extent of temperate needleleaf forest (associated with ponderosa pine forest in eastern OR) during the 21st century than MC1 (Fig. 5). Including species-specific fire resistance and realistic constraints on vegetation change owing to the legacy of existing vegetation in the STM dampens, in a biologically correct way, the frequency of vegetation shifts and results in greater vegetation resilience. On-going DGVM development includes defining new plant functional types based on physiological traits such as fire sensitivity. However physiological traits are still restricted to a handful of species, challenging the DGVM modelers to make their improvements relevant at large scales.

Despite dampening year-to-year fluctuations by using 10-year average climate (a 10-year period was used in this version of the model but could be modified to represent a longer interval), vegetation types in MC1 fluctuate sharply as climate conditions evolve. The model does not simulate realistically long lags between changes in environmental conditions and the actual replacement of the existing vegetation. This is particularly true on the West coast of the USA and the Pacific Northwest, where trees have survived for centuries despite changing climates. STMs are specifically parameterized to include empirically-defined successional trajectories that last decades to centuries unless a stand-replacement disturbance triggers a switch to a different PVT. These ecological constraints on vegetation type change are predicated on the theory that disturbance will be the catalyst for vegetation shifts with changing climate (Littell et al., 2010). Furthermore, STMs incorporate species-specific resistance to disturbance that DGVMs cannot express, since they do not simulate species. For example, with increased fire frequency in STMs, more landscape area moves into an open, large-diameter ponderosa pine state. Because ponderosa pine trees are very resistant to fire (Agee, 1993), fire does not frequently result in a state

change when it occurs in the open, large-diameter pine state. Thus, much of the area in the open, large-diameter pine state remains in that state in STM simulations. In this way, ecological constraints on vegetation type change and resistance to disturbance built into STMs can produce decade- to century-long lags in climate-induced vegetation shifts.

Climate-informed STM simulations did not show some shrublands and grasslands being as resistant to climate change as the DGVM. For example, temperate shrublands, associated with Wyoming big sage in central Oregon, declined to a greater degree by 2100 in the STM simulations than in the MC1 simulations. Temperate grasslands that could be identified locally as Bluebunch wheatgrass–Sandberg bluegrass were more abundant in MC1 than STM simulations. This was also likely due to the species-specific resistance to disturbance (or lack thereof) that was built empirically into STMs. Species that comprise shrubland and grassland communities in central Oregon are generally not as fire resistant or long-lived as many of the tree species in dry forest types; the above-ground portions of grasses and shrubs are generally killed by fire, and they recolonize via sprouting and stored or dispersed propagules. Thus, when a fire (even low-severity fire) occurs, communities shift to early-successional or open condition states, at which point available resources and lack of competition facilitate PVT shifts. Thus, we might expect similar landscapes dominated now and in the future by shrublands and grasslands to be less stable than fire-resistant dry forests, unless pest outbreaks decimate drought-stressed forests.

Although episodic shifts in vegetation were dampened in climate-informed STMs, results suggested that while there may be relative stability in vegetation conditions during the first three to four decades of the 21st century, higher volatility in vegetation conditions may occur mid-century, and stabilize again to less productive drought-adapted communities late in the 21st century. This might mean that habitat for species of interest and a variety of ecosystem services will appear relatively stable for a few decades, then experience wide swings during the following decades, a future reminiscent of the green-up/brown-down hypothesis whereby warming would first cause higher productivity in energy- (temperature) limited systems that would soon after suffer from drought conditions as warming continued and eventually caused widespread mortality.

Projected shifts in fire regimes and vegetation by climate-informed STMs are generally consistent with other projections of climate-induced change in the study region and elsewhere. For example, statistical models developed by McKenzie et al. (2004) projected that the extent of the area burned by wildfires would increase by a factor of 1.4–5 for most western states with a mean temperature increase of 2 °C. Similarly, statistical models developed by Littell et al. (2010) for the eastern Cascades in Oregon and Washington suggested that fire area burned will double or triple by the 2080s. MC1 has projected such increases at various scales over the region (Lenihan et al., 2008b; Rogers et al., 2011).

The decline in the extent of cool needleleaf forests in our simulations is consistent with a study by Littell et al. (2010) using data from Rehfeldt et al. (2006), which showed a potential decrease in the areas of climatically suitable habitat for Douglas-fir in the eastern Cascades of Washington. Douglas-fir is limited by water availability during summer at lower elevations in the Pacific Northwest (Littell et al., 2008). Increasing temperatures, lower winter snowpack, and early snowmelt with climate change will likely result in decreased summer soil moisture in parts of the Pacific Northwest (Elsner et al., 2010). Decreased summer soil moisture will likely lead to a loss of climatically suitable habitat for mesic forest types dominated by Douglas-fir east of the Cascade crest.

The continued dominance of ponderosa pine forests in the study area is consistent with a study by Coops et al. (2005) who projected the expansion of ponderosa pine on the east side of the Cascade Mountains using the 3-PG model. In contrast, Rehfeldt et al. (2006) projected decreases in the area of climatically suitable habitat for ponderosa pine in the study area. However, the climate envelope modeling approach used by Rehfeldt et al. (2006) omitted several important factors addressed by our linked model approach, including fire dependency, CO_2 fertilization effects, and biotic feedbacks.

4.1. Limitations to our approach

Our approach has several limitations:

- We have assumed that wildfire suppression will remain as effective in the future as it is currently. However, extreme fire weather may become more frequent with climate change (Abatzoglou and Brown, 2011) such that fire frequency and size may exceed our assumptions.
- The MC1 version we used for this project did not include insect outbreaks. STMs do incorporate insect outbreaks, but parameters are based on empirical data from past outbreaks, assuming similar conditions in the future. STMs could accommodate changes in the occurrence and intensity of insect or other disturbances if estimates of potential changes in future disturbance frequency and severity were readily available. On-going research in the modeling community to simulate insect population dynamics and climate-driven outbreaks will likely provide such information in the near future.
- In the STMs, we restricted PVT changes to instances when vegetation is in an early-successional or open condition or there is a stand-replacement disturbance. Thus, we did not account for PVT shifts that may occur following mixed-severity disturbances.
- We did not build in lag times for species migration in the STMs. Paleoecological records indicate that migration rates for tree species could be approximated to 200–300 m yr^{-1}, with a large associated uncertainty and species-specific response lags (Fischlin et al., 2007). We restricted all PVCs projected to occur in the three climate futures examined in this study to those that currently exist in or near to our study area, making incorporation of migration lags in the models less critical.
- We have assumed that the known dynamics of plant communities and PVTs will be relevant in the future under different climatic conditions. However, vegetation growth rates, succession rates, and species interactions are likely to change in the future.
- To link MC1 with our STMs, we in some cases represented several PVTs with a single STM, thus resulting in loss of ecological detail. This loss of ecological detail may have resulted in us missing important PVT-specific responses to changes in climate and disturbance.

Despite these limitations, results from climate-informed STMs can help to better understand potential interactions between regional-scale climate drivers, fine-scale vegetation dynamics, and shifts in disturbance regimes. Our results illustrated that legacy effects incorporated in our STM confer resilience to some plant communities under changing climate. However, results also suggested that vegetation could appear to be stable in the early part of the 21st century, then shift rapidly with increased fire and altered environmental conditions. Managers, in collaboration with scientists, can use output from this linked model process to consider potential climate-induced shifts in local vegetation conditions and develop management actions that could minimize unwanted effects of climate change. For example, in central Oregon, climate-informed STM results showed that dry ponderosa pine forests are likely to remain dominant across the landscape, but moist forests that are currently providing habitat for the northern spotted owl will likely decline. Such results can provide a base of information

for interactions between scientists and managers to strategically plan adaptive management actions (e.g., increase connectivity of late-successional forests for northern spotted owl). A forthcoming research effort will involve running different management scenarios (developed through scientist-manager collaborations) in our climate-informed STM to determine what management activities in what locations will likely maximize desirable vegetation conditions in the central Oregon study area under a changing climate.

Acknowledgments

This work was funded by the Western Wildland Environmental Threat Assessment Center, and was conducted as a part of the Integrated Landscape Assessment Project, which was funded by the American Recovery and Reinvestment Act, the USDA Forest Service Pacific Northwest Research Station, the USDA Forest Service Pacific Northwest Region, and the USDA Forest Service Southwest Region. We thank Crystal Raymond and two anonymous reviewers for their helpful suggestions to improve the manuscript.

References

Abatzoglou, J.T., Brown, T.J., 2011. A comparison of statistical downscaling methods suited for wildfire applications. International Journal of Climatology 32, 772–780.

Agee, J.K., 1993. Fire Ecology of Pacific Northwest Forests. Island Press, Washington, DC.

Allen, C.D., Macalady, A.K., Chenchouni, H., Bachelet, D., McDowell, N., Vennetier, M., Kitzberger, T., Rigling, A., Breshears, D.D., Hogg, E.H., Gonzalez, P., Fensham, R., Zhang, Z., Castro, J., Demidova, N., Lim, J., Allard, G., Running, S.W., Semerci, A., Cobb, N., 2010. A global overview of drought and heat-induced tree mortality reveals emerging climate change risks for forests. Forest Ecology and Management 259, 660–684.

Anderson, G.K., Ottmar, R.D., Prichard, S.J., 2005. CONSUME 3.0 User's Guide. USDA Forest Service, Pacific Northwest Research Station, Seattle, WA.

ApexRMS, ESSA, 2011. Path Landscape Model Online Documentation. Apex Resource Management Solutions Ltd. and ESSA Technologies Ltd., Ottawa, ON. Available at: ⟨http://wiki.pathmodel.com⟩.

Bachelet, D., Lenihan, J.M., Daly, C., Neilson, R.P., 2000. Interactions between fire, grazing and climate change at Wind Cave National Park, SD. Ecological Modelling 134, 229–244.

Bachelet, D., Lenihan, J.M., Daly, C., Neilson, R.P., Ojima, D.S., Parton, W.J., 2001. MC1, A Dynamic Vegetation Model for Estimating the Distribution of Vegetation and Associated Carbon and Nutrient Fluxes, Technical Documentation Version 1.0. General Technical Report PNW-GTR-508. USDA Forest Service, Pacific Northwest Station, Portland, OR.

Bachelet, D., Neilson, R.P., Hickler, T., Drapek, R.J., Lenihan, J.M., Sykes, M.T., Smith, B., Sitch, S., Thonicke, K., 2003. Simulating past and future dynamics of natural ecosystems in the United States. Global Biogeochemical Cycles 17, 1045.

Cohen, J.D., Deeming, J.E., 1985. The National Fire-Danger Rating System: Basic Equations. General Technical Report PSW-GTR-82. USDA Forest Service Pacific Southwest Research Station, Berkeley, CA.

Coops, N.C., Waring, R.H., Law, B.E., 2005. Assessing the past and future distribution and productivity of ponderosa pine in the Pacific Northwest using a process model, 3-PG. Ecological Modelling 183, 107–124.

Cramer, W., Bondeau, A., Woodward, F.I., Prentice, E., Betts, R.A., Brovkin, V., Cox, P.M., Fisher, V., Foley, J.A., Friend, A.D., Kucharik, C., Lomas, M.R., Ramankutty, N., Sitch, S., Smith, B., White, A., Young-Molling, C., 2001. Global response of terrestrial ecosystem structure and function to CO_2 and climate change: results from six global dynamic vegetation models. Global Change Biology 7, 357–373.

Crookston, N.L., Finley, A.O., 2007. yaImpute: an R package for *k*-NN imputation. Journal of Statistical Software 23, 1–16.

Daly, C., Bachelet, D., Lenihan, J.M., Neilson, R.P., Parton, W., Ojima, D., 2000. Dynamic simulation of tree–grass interactions for global change studies. Ecological Applications 10, 449–469.

Daly, C., Halbleib, M., Smith, J.I., Gibson, W.P., Doggett, M.K., Taylor, G.H., Curtis, J., Pasteris, P.P., 2008. Physiographically sensitive mapping of climatological temperature and precipitation across the conterminous United States. International Journal of Climatology 28, 2031–2064.

Daly, C., Taylor, G.H., Gibson, W.P., 1997. The PRISM approach to mapping precipitation and temperature. In: Proceedings of the 10th American Meteorological Society Conference on Applied Climatology. American Meteorological Society, Reno, NV, pp. 10–12.

Eidenshink, J., Schwind, B., Brewer, K., Zhu, Z.L., Quayle, B., Howard, S., 2007. A project for monitoring trends in burn severity. Fire Ecology 3, 3–20.

Elsner, M.M., Cuo, L., Voisin, N., Deems, J.S., Hamlet, A.F., Vano, J.A., Mickelson, K.E.B., Lee, S., Lettenmaier, D.P., 2010. Implications of 21st century climate change for the hydrology of Washington State. Climatic Change 102, 225–260.

ESSA Technologies Ltd., 2007. Vegetation Dynamics Development Tool User Guide, Version 6.0. Vancouver, British Columbia.

Evers, L., 2010. Modeling Sage-grouse Habitat Using a State-and-Transition Model. Ph.D. Dissertation. Oregon State University, Corvallis, OR.

Fischlin, A., Midgley, G.F., Price, J.T., Leemans, R., Gopal, B., Turley, C., Rounsevell, M.D.A., Dube, O.P., Tarazona, J., Velichko, A.A., 2007. Ecosystems, their properties, goods, and services. In: Parry, M.L., Canziani, O.F., Palutikof, J.P., van der Linden, P.J., Hanson, C.E. (Eds.), Climate Change: Impacts, Adaptation, and Vulnerability: Contribution of Working Group II to the Fourth Assessment Report of the Intergovernmental Panel on Climate Change. Cambridge University Press, Cambridge, UK, pp. 211–272.

Foley, J.A., Levis, S., Prentice, I.C., Pollard, D., Thompson, S.L., 1998. Coupling dynamic models of climate and vegetation. Global Change Biology 4, 561–579.

Forbis, T.A., Provencher, L., Frid, L., Medlyn, G., 2006. Great Basin land management planning using ecological modeling. Environmental Management 38, 62–83.

Fowler, H.J., Blenkinsop, S., Tebaldi, C., 2007. Linking climate change modeling to impacts studies: recent advances in downscaling techniques for hydrological modeling. International Journal of Climatology 27, 1547–1578.

Friedlingstein, P., Fung, I., Holland, E., John, J., Brasseur, G., Erickson, D., Schimel, D., 1995. On the contribution of CO_2 fertilization to the missing biospheric sink. Global Biogeochemical Cycles 9, 541–556.

Gonzalez, P., Neilson, R.P., Lenihan, J.M., Drapek, R.J., 2010. Global patterns in the vulnerability of ecosystems to vegetation shifts due to climate change. Global Ecology and Biogeography 19, 755–768.

Gordon, C., Cooper, C., Senior, C.A., Banks, H.T., Gregory, J.M., Johns, T.C., Mitchell, J.F.B., Wood, R.A., 2000. The simulation of SST, sea ice extents and ocean heat transports in a version of the Hadley Centre coupled model without flux adjustments. Climate Dynamics 16, 147–168.

Gordon, H.B., Rotstayn, L.D., McGregor, J.L., Dix, M.R., Kowalczyk, E.A., Farrell, S.P., Waterman, L.J., Hirst, A.C., Wilson, S.G., Collier, M.A., Watterson, I.G., Elliott, T.I., 2002. The CSIRO Mk3 Climate System Model. CSIRO Atmospheric Research Technical Paper No. 60. CSIRO Atmospheric Research.

Halofsky, J.E., Peterson, D.L., O'Halloran, K.A., Hawkins Hoffman, C. (Eds.), 2011. Adapting to Climate Change at Olympic National Forest and Olympic National Park. General Technical Report PNW-GTR-844. USDA Forest Service, Pacific Northwest Research Station, Portland, OR.

Hann, W.J., Jones, J.L., Karl, M.G., Hessburg, P.F., Keane, R.E., Long, D.G., Menakis, J.P., McNicoll, C.H., Leonard, S.G., Gravenmier, R.A., Smith, B.G., 1997. Landscape Dynamics of The Basin. In: Quigley, T.M., Arbelbide, S.J. (Eds.), An Assessment of Ecosystem Components in the Interior Columbia Basin and Portions of the Klamath and Great Basins. General Technical Report PNW-GTR-405. USDA Forest Service, Pacific Northwest Research Station, Portland, OR, pp. 337–1055.

Hasumi, H., Emori, S. (Eds.), 2004. K-1 Coupled Model (MIROC) Description. Technical Report 1. University of Tokyo, Center for Climate System Research, Tokyo.

Hayhoe, K., Cayan, D., Field, C., Frumhoff, P., Maurer, E., Miller, N., Moser, S., Schneider, S., Cahill, K., Cleland, E., Dale, L., Drapek, R., Hanemann, R., Kalkstein, L., Lenihan, J., Lunch, C., Neilson, R., Sheridan, S., Verville, J., 2005. Emission pathways, climate change, and impacts on California. Proceedings of the National Academy of Sciences 101, 12422–12427.

Hemstrom, M.A., Korol, J.J., Hann, W.J., 2001. Trends in terrestrial plant communities and landscape health indicate the effects of alternative management strategies in the interior Columbia River basin. Forest Ecology and Management 153, 105–125.

Hemstrom, M.A., Merzenich, J., Reger, A., Wales, B., 2007. Integrated analysis of landscape management scenarios using state and transition models in the upper Grande Ronde River Subbasin, Oregon, USA. Landscape and Urban Planning 80, 198–211.

Hemstrom, M.A., Wisdom, M.J., Hann, W.J., Rowland, M.M., Wales, B.C., Gravenmier, R.A., 2002. Sagebrush-steppe vegetation dynamics and restoration potential in the Interior Columbia Basin, U.S.A. Conservation Biology 16, 1243–1255.

Hickler, T., Smith, B., Sykes, M.T., Davis, M.B., Sugita, S., Walker, K., 2004. Using a generalized vegetation model to simulate vegetation dynamics in northeastern USA. Ecology 85, 519–530.

Horn, H.S., 1975. Markovian properties of forest succession. In: Cody, M.L., Diamond, J.M. (Eds.), Ecology and Evolution of Communities. Harvard University Press, Cambridge, MA, pp. 196–211.

IPCC [Intergovernmental Panel on Climate Change], 2007. In: Solomon, S., Qin, D., Manning, M., Chen, Z., Marquis, M., Avery, K.B., Tignor, M., Miller, H.L. (Eds.), Contribution of Working Group I to the Fourth Assessment Report of the Intergovernmental Panel on Climate Change. Cambridge University Press, Cambridge and New York.

Johns, T.C., Gregory, J.M., Ingram, W.J., Johnson, C.E., Jones, A., Lowe, J.A., Mitchell, J.F.B., Roberts, D.L., Sexton, D.M.H., Stevenson, D.S., Tett, S.F.B., Woddage, M.J., 2003. Anthropogenic climate change for 1860 to 2100 simulated with the HadCM3 model under updated emissions scenarios. Climate Dynamics 20, 583–612.

Laycock, W.A., 1991. Stable states and thresholds of range condition on North American rangelands: a viewpoint. Journal of Range Management 44, 427–433.

Lenihan, J.M., Bachelet, D., Neilson, R.P., Drapek, R., 2008a. Response of vegetation distribution, ecosystem productivity, and fire to climate change scenarios for California. Climatic Change 87 (Suppl 1), S215–S230.

Lenihan, J.M., Bachelet, D., Neilson, R.P., Drapek, R.J., 2008b. Simulated response of conterminous United States ecosystems to climate change at different levels of fire suppression, CO_2 emission rate, and growth response to CO_2. Global and Planetary Change 64, 16–25.

Lenihan, J.M., Daly, C., Bachelet, D., Neilson, R.P., 1998. Simulating broad-scale fire severity in a dynamic global vegetation model. Northwest Science 72, 91–103.
Lenihan, J.M., Drapek, R.J., Bachelet, D., Neilson, R.P., 2003. Climate changes effects on vegetation distribution, carbon, and fire in California. Ecological Applications 13, 1667–1681.
Littell, J.S., Oneil, E.E., McKenzie, D., Hicke, J.A., Lutz, J.A., Norheim, R.A., Elsner, M.M., 2010. Forest ecosystems, disturbance, and climatic change in Washington State, USA. Climatic Change 102, 129–158.
Littell, J.S., Peterson, D.L., Tjoelker, M., 2008. Douglas-fir growth in mountain ecosystems: water limits tree growth from stand to region. Ecological Monographs 78, 349–368.
McKenzie, D.H., Gedalof, Z., Peterson, D.L., Mote, P., 2004. Climatic change, wildfire, and conservation. Conservation Biology 18, 890–902.
Merzenich, J., Kurz, W.A., Beukema, S., Arbaugh, M., Schilling, S., 2003. Determining forest fuel treatments for the Bitterroot front using VDDT. In: Arthaud, G.J., Barrett, T.M. (Eds.), Systems Analysis in Forest Resources. Kluwer Academic Publishers, Dordrecht, pp. 47–59.
Mitchell, T.D., Carter, T.R., Jones, P.D., Hulme, M., New, M., 2004. A Comprehensive Set of High-Resolution Grids of Monthly Climate for Europe and the Globe: The Observed Record (1901–2000) and 16 Scenarios (2001–2100). University of East Anglia, Norwich, UK.
Mote, P.W., Salathé Jr., E.P., 2010. Future climate in the Pacific Northwest. Climatic Change 102, 29–50.
Nakićenović, N., Swart, R. (Eds.), 2000. Special Report on Emissions Scenarios. A Special Report of Working Group III of the Intergovernmental Panel on Climate Change. Cambridge University Press, Cambridge and New York.
Neilson, R.P., 1995. A model for predicting continental-scale vegetation distribution and water balance. Ecological Applications 5, 362–385.
Noble, I.R., Slatyer, R.O., 1980. The use of vital attributes to predict successional changes in plant communities subject to recurrent disturbances. Vegetatio 43, 5–21.
Ohmann, J., Gregory, M.J., 2002. Predictive mapping of forest composition and structure with direct gradient analysis and nearest neighbor imputation in coastal OR, USA. Canadian Journal of Forest Research 32, 725–741.
Omernik, J.M., 1987. Ecoregions of the coterminous United States. Annals of the Association of American Geographers 77, 118–125.
Parmesan, C., 2006. Ecological and evolutionary responses to recent climate change. Annual Review of Ecology, Evolution, and Systematics 37, 637–669.
Parton, W.J., Scurlock, J.M.O., Ojima, D.S., Gilmanov, T.G., Scholes, R.J., Schimel, D.S., Kirchner, T., Menaut, J.C., Seastedt, T., Garcia Moya, E., Kamnalrut, A., Kinyamario, J.I., 1993. Observations and modeling of biomass and soil organic matter dynamics for the grassland biome worldwide. Global Biogeochemical Cycles 7, 785–809.
Peterson, D.L., Ryan, K.C., 1986. Modeling postfire conifer mortality for long-range planning. Environmental Management 10, 797–808.
Prentice, I.C., Bondeau, A., Cramer, W., Harrison, S., Hickler, T., Lucht, W., Sitch, S., Smith, B., Sykes, M., 2007. Dynamic global vegetation modeling: quantifying terrestrial ecosystem responses to large-scale environmental change. In: Canadell, J.G., Pataki, D., Pitelka, L.F. (Eds.), Terrestrial Ecosystems in a Changing World. Springer-Verlag, Berlin, pp. 175–192.
Prentice, I.C., Webb, R.S., Ter-Mikhaelian, M.T., Solomon, A.M., Smith, T.M., Pitovranov, S.E., Nikolov, N.T., Minin, A.A., Leemans, R., Lavorel, S., Korzukhin, M.D., Helmisaari, H.O., Hrabovszky, J.P., Harrison, S.P., Emanuel, W.R., Bonan, G.B., 1989. Developing a Global Vegetation Dynamics Model: Results of an IIASA Summer Workshop. Research Report RR-89-7. International Institute for Applied Systems Analysis, Laxenburg.
PRISM Group, 2012. Parameter-elevation Regressions on Independent Slopes Model Climate Mapping System. Available at: http://www.prism.oregonstate.edu/
Provencher, L., Anderson, T., 2011. Climate Change Revisions to Nevada's Wildlife Action Plan: Vegetation Mapping and Modeling Report to the Nevada Department of Wildlife. The Nature Conservancy, Reno, NV.
Rehfeldt, G.E., Crookston, N.L., Warwell, M.V., Evans, J.S., 2006. Empirical analysis of plant-climate relationships for the western United States. International Journal of Plant Sciences 167, 1123–1150.
Rogers, B.M., Neilson, R.P., Drapek, R., Lenihan, J.M., Wells, J.R., Bachelet, D., Law, B.E., 2011. Impacts of climate change on fire regimes and carbon stocks of the U.S. Pacific Northwest. Journal of Geophysical Research 116, G03037.
Rothermel, R., 1972. A Mathematical Model for Fire Spread Predictions in Wildland Fuels: Research Paper INT-RP-115. USDA Forest Service, Ogden, UT.
Shaw, M.R., Pendleton, L., Cameron, D.R., Morris, B., Bachelet, D., Klausmeyer, K., MacKenzie, J., Conklin, D.R., Bratman, G.N., Lenihan, J., Haunreiter, E., Daly, C., Roehrdanz, P.R., 2011. The impact of climate change on California's ecosystem services. Climatic Change 109 (Suppl 1), S465–S484.
The Nature Conservancy, USDA Forest Service, and Department of the Interior, 2006. LANDFIRE Vegetation Dynamics Modeling Manual, Version 4.1. Boulder, CO.
van Wagner, C.E., 1973. Height of crown scorch in forest fires. Canadian Journal of Forest Research 3, 373–378.
Weisz, R., Triepke, J., Truman, R., 2009. Evaluating the ecological sustainability of a ponderosa pine ecosystem on the Kaibab Plateau in northern Arizona. Fire Ecology 5, 100–114.
Westerling, A.L., Hidalgo, H.G., Cayan, D.R., Swetnam, T.W., 2006. Warming and earlier spring increase western U.S. forest wildfire activity. Science 313, 940–943.
Westoby, M., Walker, B., Noy-Meir, I., 1989. Opportunistic management for rangelands not at equilibrium. Journal of Range Management 42, 266–276.